Applied Surface Science 581 (2022) 152292

Contents lists available at ScienceDirect

Applied Surface Science

journal homepage: www.elsevier.com/locate/apsusc

Full Length Article

Depth profiling of thin plasma-polymerized amine films using GDOES in an Ar-O_2 plasma

Janez Kovač [a,*], Jernej Ekar [a,b], Miha Čekada [c], Lenka Zajíčková [d,e], David Nečas [f], Lucie Blahová [d], Jiang Yong Wang [g], Miran Mozetič [a]

[a] Department for Surface Engineering, Jozef Stefan Institute, Jamova cesta 39, Ljubljana SI 1000, Slovenia
[b] Jozef Stefan International Postgraduate School, Jamova cesta 39, Ljubljana SI 1000, Slovenia
[c] Department of Thin Films and Surfaces, Jozef Stefan Institute, Jamova cesta 39, Ljubljana SI 1000, Slovenia
[d] Central European Institute of Technology – CEITEC, Brno University of Technology, Purkyňova 123, Brno 61200, Czech Republic
[e] Department of Condensed Matter Physics, Faculty of Science, Masaryk University, Kotlářská 2, Brno 61200, Czech Republic
[f] Central European Institute of Technology – CEITEC, Brno University of Technology, Purkyňova 123, Brno 61200, Czech Republic
[g] Department of Physics, Shantou University, 243 Daxue Road, Shantou, Guangdong 515063, China

ARTICLE INFO

Keywords:
GDOES
Depth profile
Amine plasma polymer
Ar-O_2 plasma

ABSTRACT

Thin polymer films were deposited on polished stainless-steel samples by PECVD from a cyclopropylamine precursor and characterized by X-ray photoelectron spectroscopy, secondary-ion mass spectrometry and glow-discharge optical emission spectroscopy (GDOES) depth profiling. These depth profiles exhibited reasonable agreement. The GDOES involved the erosion of the polymer films in plasma sustained by an asymmetric RF capacitively coupled discharge using both Ar and Ar-O_2 gases. The application of pure Ar caused unwanted effects, such as the broadening of the polymer-film/substrate interface, which were suppressed when using the mixture with oxygen. Another benefit of oxygen was a significant increase in the etching rate by a factor of about 15 as compared to pure argon. The mechanisms involved in the depth profiling using the mixture of gases were elaborated in some detail, taking into account plasma parameters typical for an asymmetric, capacitively coupled RF discharge in a small volume. The main benefit of using the Ar/O_2 GDOES profiling with respect to XPS and SIMS depth profiling is the increased sputtering rate for polymer films. Comparing the GDOES depth profiling with the Ar/O_2 mixture with profiling in pure Ar, the benefits are a higher sputtering rate and better depth resolution at the polymer/substrate interface.

1. Introduction

Glow-discharge optical emission spectroscopy (GDOES) is a technique used for the depth profiling of thin films. It was developed about 50 years ago [1], and the first commercial instrument was developed in the 1980 s. A review of this technique, summarizing developments up to 2005, was prepared by Hoffmann et al. [2]. GDOES enables the rapid depth profiling of a variety of samples. Compared to other techniques that only operate well in ultra-high-vacuum conditions, such as Auger electron spectroscopy (AES), X-ray photoelectron spectroscopy (XPS) and secondary-ion mass spectrometry or secondary-neutral mass spectrometry (SIMS and SNMS, respectively), GDOES operates well at a medium pressure of the order of 100 Pa. The ion current used for sputtering the samples is thus much larger in GDOES than in these other techniques, and so is the sputtering rate. The classic techniques for depth profiling involve a sputtering rate of the order of nm/s, while GDOES operates at an order of magnitude higher rate. The acquisition of optical lines arising from atomic transitions is almost instant due to the sophisticated optical spectrometer. Traditional GDOES instruments employ direct-current (DC) discharges as the ion sources, but advanced versions are equipped with radio-frequency (RF) discharges. The advantage of RF discharges is that an electric current in the frequency range of the order of MHz also flows through any dielectric material placed on the powered electrode, so such versions are also suitable for the depth profiling of insulators, providing their thickness is reasonable. Modern instruments allow for pulsed RF discharges.

Despite the possibility to etch dielectrics, the literature on the GDOES depth profiling of polymer films is scarce. Carquigny et al. [3]

* Corresponding author.
E-mail address: janez.kovac@ijs.si (J. Kovač).

https://doi.org/10.1016/j.apsusc.2021.152292
Received 6 July 2021; Received in revised form 1 December 2021; Accepted 18 December 2021
Available online 28 December 2021

used this technique for the characterization of thin polypyrrole films loaded with dopants for pharmaceutical applications. She employed a flush time of 500 s, an argon pressure of 400 Pa, and discharge power of 20 W. The thickness of the polymer films prepared by electrodeposition was of the order of 10 μm, and the acquisition of the GDOES depth profile took about 10 min. Similar material was deposited with a comparable technique by Cysewska et al. [4], and the depth-profile acquisition time was also about 10 min. Similar results with doped polypyrrole films were also reported by Sizun et al. [5]. Giaveri et al. [6] prepared thin films of doped polysiloxane-epoxy resin with a thickness of about 50 μm and determined the composition of such coatings, which are useful as high-temperature corrosion-protection coatings. A detailed study of the GDOES characterization of thin polymer films was reported by Moutarlier et al. [7]. They deposited polyaniline films by electrochemical methods and characterized them thoroughly by GDOES. They used a flush time of 60 s, a discharge power of 10 W, and discharge pressure of 400 Pa. They found these parameters to be the most suitable for depth profiling. The thickness of the deposited films as determined by profilometry was between 0.7 and 7 μm. Relatively porous polymer films were obtained with a roughness of approximately 100 nm. The depth profiles were acquired in a few minutes. Groza et al. studied different polymer-composite layers of doped hydroxyapatite polydimethylsiloxanes with a thickness below 1 μm using GDOES at a pressure of 650 Pa, a RF discharge power of 35 W in pulsed mode at a pulse frequency of 1 kHz and a duty cycle of 0.25 [8]. Surmeian et al. [9] applied both GDOES and glow-discharge time-of-flight mass spectrometry (GD-TOFMS) to study the depth profiles of polymer films. The films for GDOES were sputtered at a discharge pressure of 650 Pa, 25 W of RF power operating in pulsed mode at 3 kHz, and a duty cycle of 0.25. For GD-TOFMS the authors found suitable parameters, i.e., 700 Pa of pressure and 30 W of RF power in the pulsed mode with a pulse duration of 1 ms and a period of 4 ms. Mass spectra were recorded over the entire pulse duration and thereby also in the plasma afterglow. The above-cited researchers always sustained gaseous plasma in the GDOES in pure argon. GDOES depth profiling was applied by Y. Liu et al. to very thin organic films like a self-assembled thiourea layer on copper. The authors showed that by using the MRI (mixing-roughness-information depth) model for GDOES depth profiling, a very good depth resolution (Δz as low as 0.5 nm) could be obtained [10]. Although some GDOES devices also allow a mixture of argon and oxygen for the depth profiling of samples, there are not many scientific papers investigating this topic. In two papers, Fernandez et al. studied the influence of hydrogen, nitrogen, and oxygen additions to argon for RF-GDOES depth profiling [11,12]. They found a decrease in the sputtering rate when adding oxygen to argon, as compared with pure argon. They also reported a great potential to improve the depth resolution for thin-film depth profiling when using gas mixtures. Takahara et al. studied the influence of small quantities of oxygen and hydrogen to argon on GDOES depth profiling of graphite electrodes in lithium-ion batteries. They discussed profile analysis, both its speed and quality. They found that adding oxygen to argon plasma increased the sputtering rate on the graphite layer but the chemical etching was more inhomogeneous in this case [13]. Fischer et al. studied the influence of controlled addition of N_2 and of O_2 to Ar on the sputtering rate, the emission intensity of spectral lines in a DC glow discharge for bulk samples of the pure metals Al, Ti, Fe, Ni, Cu, and Ag. The effect of the gaseous addition was a decrease in the sputtering rate of metals with increasing concentrations of N_2 or O_2 [14].

The scientific literature on gaseous plasma created in oxygen-containing gas mixtures with a high-frequency discharge is abundant, and so is the literature on the interaction of such plasma with polymer materials. Recent review papers such as [15], [16] and [17] summarize the advances in both scientific niches and provide suitable references. Of particular relevance are papers reporting the behavior of plasma sustained in a mixture of argon and oxygen at a discharge power density similar to that applied in modern RF-driven GDOES instruments. A complete description of gaseous plasma sustained in a tube filled with Ar-O_2 was prepared by Kutasi et al. [18]. They included over 100 reactions occurring in the gas mixture depending on plasma conditions. The discharge tube was 5 mm in diameter and the power density of the order of 10 W/cm^3, similar to the discharges employed in RF-driven GDOES. They found the dissociation fraction of oxygen molecules close to 50% at a pressure of several 100 Pa and an oxygen concentration in the gas mixture of 4%. The dissociation fraction decreased with increasing probability for the heterogeneous surface recombination of O atoms to parent molecules. At a recombination coefficient of 0.01, the dissociation fraction was about 35% at a pressure of 267 Pa, with 5% of oxygen in the Ar-O_2 mixture. For a coefficient of 0.1, the dissociation fraction was much lower than about 5%. In general, the O-atom density was of the order of 10^{21} in this gas mixture. Therefore, orders of magnitude larger than the density of any ions. The ion densities were much lower, of the order of 10^{17} m^{-3} for Ar^+, 10^{16} m^{-3} for O^+, and 10^{15} m^{-3} for $O_2{}^+$. The density of Ar metastables was of the order of 10^{17} m^{-3}. These data represent an important estimation of the plasma parameters in the discharge tube of a modern GDOES driven by an RF discharge.

In this work, we addressed the important challenges in the field of plasma polymer interactions like the synergy of the ion sputtering and the reactive chemical etching of polymer by the oxygen addition in the Ar-plasma applied in GDOES configuration. We report experiments performed using both pure argon and a mixture of Ar + 4 vol% of O_2 for GDOES depth profiling at various discharge parameters like power and gas pressure. We discuss the results in terms of the scientific literature on the interaction of Ar-O_2 plasma with polymer materials. We also addressed artifacts and interface broadening observed by GDOES depth profiling of polymer layer in pure Ar and Ar/O_2 mixture. The beneficial results when using oxygen are emphasized. Further, we compare GDEOS depth profiling of the polymer layer with the ToF-SIMS and XPS depth profiling of such layer. We believe that such a systematic study of GDOES etching of polymer by the Ar/O_2 mixture has not yet been reported.

The polymer film characterized in our study is a plasma polymerized cyclopropylamine film. This film contains a high concentration of amine groups, and it is of high interest for tissue engineering. The PP-CPA-coated surfaces exhibited extremely high cell adhesion [19]. A possibility for many applications of CPA films was a reason to select this polymer for systematic investigation of GDOES depth profiling. We believe that the results of our study may also be applied to other types of polymers.

2. Experimental details

Thin films containing amino groups were prepared by plasma-enhanced chemical vapor deposition (PECVD) on commercially available, polished, stainless-steel substrates with a thickness of 0.75 mm. The substrates were cut into rectangular pieces with dimensions of 10 cm × 5 cm and carefully cleaned. They were put on the bottom electrode of a high-vacuum PECVD chamber in which a capacitively coupled plasma discharge was ignited at 13.56 MHz between two parallel-plate electrodes. The chamber was a stainless-steel cylinder, 490 mm in inner diameter and 246 mm in height, closed by two stainless-steel flanges. The bottom electrode, 420 mm in diameter, was connected to a radio-frequency (RF) generator via a matching unit containing a blocking capacitor. Thus, the bottom electrode with substrates was negatively DC self-biased depending on the applied RF power and the pressure. Details of this relation can be found in our previous publications [20,21,19]. The processing gas, either argon for the substrate cleaning or Ar with cyclopropylamine vapors (CPA, C_3H_7N) for the deposition, was fed into the chamber through a grounded upper showerhead electrode, 380 mm in diameter. The distance between the electrodes was 55 mm. A sketch of the experimental setup is shown in Ref. [19].

The PECVD chamber was evacuated with a turbomolecular pump backed with a two-stage rotary pump to an ultimate pressure of 1×10^{-4} Pa. The system was not baked but evacuated for 20 h before depositing

the coating. The pressure during both processes (the substrate cleaning and the thin-film deposition) was adjusted to 50 Pa with a valve between the chamber and the turbomolecular pump. The Ar flow rate of 28 sccm was regulated with an electronic flow controller, whereas the flow rate of CPA vapor was set to 2 sccm with a needle valve. Thus, the effective pumping speed during the deposition was only about 1 l/s, which was found to be helpful for increasing the residence time of gaseous precursors inside the reaction chamber and thus the optimal formation of radicals from CPA for the deposition of high-quality films. Before the deposition, the substrates were sputter-cleaned for 5 min with a pulsed Ar plasma at 100 W (33 % duty cycle, 500-Hz pulse repetition frequency). The plasma polymerization of CPA was also carried out in the pulsed mode (33 % duty cycle and 500-Hz repetition frequency) at 100 W on-time RF power. The applied optimized conditions of the CPA plasma polymerization yielded stable yet amine-rich films, as found previously [21]. Different deposition times were chosen (12, 24, and 96 min) to obtain thin films of different thicknesses. The films were characterized by spectroscopic ellipsometry, and the thicknesses obtained by the fitting were 70.2 ± 0.4 nm, 118.2 ± 1.3 nm, and 502 ± 3 nm, respectively. The deposition rate corresponding to these three films vary within the statistical variations observed for a large number of deposition experiments. However, the film composition was not influenced by these variations.

The samples were characterized by XPS, ToF-SIMS, AFM, and GDOES. The XPS analyses were carried out with the PHI-TFA XPS spectrometer (Physical Electronics Inc) using a monochromatized X-ray Al source. The analyzed area was 0.4 mm in diameter. The surface composition was quantified from the XPS peak intensities, taking into account the instrument manufacturer's relative sensitivity factors. The XPS analyses were performed in combination with ion sputtering to analyse the depth distribution of the elements in the sub-surface region. The Ar ions with an energy of 3 keV were used for rastering an area of 3 × 3 mm^2. During the XPS depth profiling, the signals of C 1 s, N 1 s, O 1 s, Fe 2p, Cr 2p, and Ni 2p were acquired. The pass energy of the electron analyser was 187 eV for the acquisition of the XPS spectra during the depth profiling and 29 eV for the acquisition of the XPS spectra from the surface.

ToF-SIMS analyses were performed using a ToF–SIMS 5 instrument (ION-TOF, Münster, Germany) equipped with a bismuth liquid–metal ion gun with a kinetic energy of 30 keV. The analyses were performed in an ultra-high vacuum of approximately 10^{-7} Pa. The SIMS spectra of the negative ions were measured by scanning a Bi^+ cluster ion beam over an area 100 × 100 μm^2 in size. The beam current was 0.6 pA, and the total measuring time to acquire the SIMS spectra was 500 s. The dose of the primary ions during the measurements was in the static regime. An electron gun was used to prevent charge compensation on the sample surfaces during the analysis. The SIMS depth profile was obtained in dual-beam mode using a Bi^+ beam as the analyzing beam and a Cs^+ beam at 0.5 keV for sputtering. The sputtering rate was about 0.42 nm/s. During the ToF-SIMS depth profiling, the analyses chamber was flooded by H_2 gas at the pressure of $7x10^{-5}$ Pa to reduce the matrix effect.

AFM measurements were made on polymer films that were sputtered to half of the film's thickness to reveal the surface morphology. A Dimension Icon AFM instrument, produced by Brucker, was employed in semi-contact mode for these measurements. The surface morphology of the bottom of the craters after GDOES depth profiling was examined by stylus profilometer (Taylor Hobson Talysurf).

The GDOES depth profiling was performed in the pulsed RF GDOES instrument, GD-Profiler 2 by Horiba Scientific. This instrument integrated the ultra-fast sputtering mode (UFS) based on applying a mixture of gases during the depth profiling, as patented by Horiba Scientific [22]. The GD plasma excited at 13.56 MHz was confined within the non-biased copper tube of 4 mm in diameter. The GDOES depth profiling was performed at different powers from 20 to 45 W and at different pressures from 400 to 700 Pa. The RF power was pulsed with a frequency of 2.5 kHz and a duty cycle of 25%. A pure Ar gas and a mixture of 96 vol% Ar and 4 vol% O_2 gases were used for the sputtering during the depth profiling. Optical transitions were recorded in the spectral range 100–800 nm.

The GDOES had a powerful plasma for sputtering the sample surface, so heating of the uppermost layer is expected during the depth profiling. The surface layer's temperature can be estimated from the known discharge power, taking into account some assumptions. The GDOES employs a highly asymmetrical, capacitively coupled RF discharge. Such discharges are characterized by an asymmetrical distribution of the power applied to the electrodes: the major fraction is dissipated at the smaller electrode. Such a configuration is beneficial since the voltage drop between the plasma and the smaller electrode is much higher than in the large electrode's plasma sheath. Consequently, the positive ions accelerate in the plasma sheath at the small electrode to high kinetic energy. They create collision cascades with atoms in the samples' surface layer, releasing their kinetic energy, i.e., heating the surface layer with a thickness of the order of the ion-penetration depth. The penetration depth of such ions is several nm, so one can assume all the available RF power is dissipated on the surface of the sample. A temperature gradient is thus established across the sample. Assuming further infinite thermal conductivity of the sample holder, the difference in temperature between the sample surface facing the plasma and the rear in steady conditions (i.e., neglecting the thermal capacity of the sample) is calculated using a simple equation

$$\Delta T = \frac{P}{S}\left(\frac{d_{steel}}{\lambda_{steel}} + \frac{d_{polymer}}{\lambda_{polymer}}\right) \quad (1)$$

Here, P is the discharge power, d is the sample thickness, λ is the thermal conductivity, and S is the area of the sample facing the plasma. Assuming the sample holder is kept at 300 K at all times, the temperature of the sample surface is shown versus the thickness of the polymer layer in Fig. 1 for the case of discharge power of 30 W, a sample diameter of 5 mm, and for a stainless-steel substrate with a thickness of 0.75 mm. Namely, our samples were polymer films on stainless-steel substrates. The thermal conductivities (λ) of the polymer film and the stainless-steel substrate were taken as 0.5 W/(m K) and 15 W/(m K), respectively.

The temperatures plotted in Fig. 1 are definitely overestimated since not all the discharge power is dissipated on the sample surface. Still, Fig. 1 is useful for estimating any thermal effects. As can be seen in Fig. 1, the expected surface temperature is between 100 and 400 °C. In our case, there is a thin film of polymer on the stainless-steel substrate with a thickness of 0.75 mm. Since the stainless steel has only moderate thermal conductivity, the surface temperature as calculated with equation (1) is not negligible – about 100 °C for the stainless-steel substrate with a thickness of 0.75 mm. The thickness of the polymer film in our case is up to 0.5 μm, so the temperature gradient across the polymer film

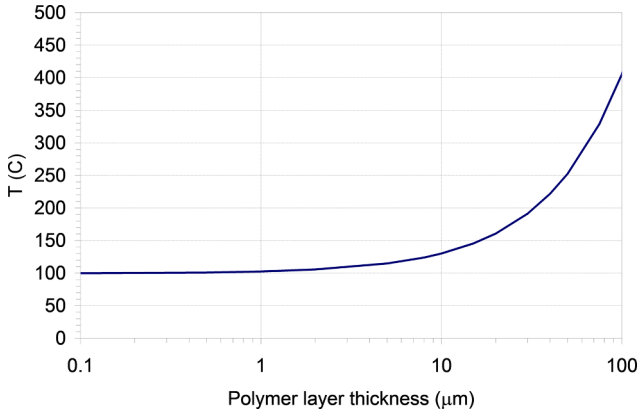

Fig. 1. The temperature of the sample surface consisting of the polymer layer of variable thickness on the steel foil of 0.75 mm in thickness upon depth profiling by GDOES at discharge power 30 W.

due to exposure to gaseous plasma is negligible – up to a couple of °C. In any case, the results of the simple calculation confirm that the surface of the polymer sample in our case does not heat to a temperature where the thermal decomposition of the polymer film would become significant. Still, we should be aware of thermal effects if thicker polymer films were used. For example, the surface of a polymer foil of thickness 0.1 mm would heat to over 400 °C. This has to be taken into account when probing thick samples that have poor thermal conductivity using the GDOES technique.

3. Results and discussion

Detailed XPS analyses of the surface of the plasma-polymerized polyamine film studied here have already been reported [19,23,24]. The film composition averaged over several deposition experiments was 79.5 ± 1.0 at.% of C, 17.2 ± 0.5 at.% of N and 3.3 ± 0.8 at.% of O, as measured maximum three days after the deposition. The XPS analyses performed in the present study were carried out more than one month after the deposition, and, therefore, the concentration of oxygen at the film surface was higher due to a film oxidation. Namely, the composition was 80 at.% C, 11 at.% N and 9 at.% O.

We focused on the XPS depth profiling of an amine film. Fig. 2 shows an XPS depth profile of the amine film with a thickness of 70 nm. The sputtering time to acquire the total depth profile was 1.5 h. We estimated the sputtering rate to be 2.0 nm/min for this polymer film. We did not attempt to acquire XPS depth profiles for thicker polymer films since the analysis time would be very long. For the 1-μm-thick films, the required analysis time would be almost one day.

The depth profile in Fig. 2 reveals some details that are worth discussing. First, the oxygen concentration dropped quickly to 2 at.% after starting to etch the polymer film. A decrease of nitrogen (to 6 at.%) was also observed. A possible explanation for these changes is a preferential sputtering of these two elements with Ar ions [25]. The artifact due to preferential etching of N and O upon depth profiling with a monoatomic Ar ion gun can be partially avoided using more sophisticated Ar-cluster ions optimized for etching the polymer films [26]. However, we believe that the significant decrease in the amount of oxygen, the concentration of which stabilized at 1–2 at.% through the polymer film's entire thickness, is also related to the depth-limited amine film oxidation. Here, it is worth mentioning that monochromatic Ar sputtering also causes partial de-hydrogenation of polymers, which may further influence the composition as deduced from XPS depth profiles.

The interface width between the polymer film and the stainless-steel substrate in the XPS depth profile shown in Fig. 2 is about 15 nm. The measured interface width may be related to the analyses depth of the XPS method, which may be up to 10 nm, or the atom mixing at the interface induced by the ion sputtering. The main reason for the interface width measured by XPS is probably related to the surface roughness of the steel substrate, considering that the as-received stainless-steel sheets were not additionally polished. The interface is enriched with oxygen that is explained by weak oxidation of the stainless-steel substrate. The cleaning by bombardment with Ar ions performed in-situ before polymer film deposition was not efficient enough to remove the native oxide film. Still, the concentration of oxygen within the interface is only several at.%.

The sample with the 70-nm-thick polymer films was also characterized by ToF-SIMS. A typical depth profile of negative secondary ions obtained by sputtering with the Cs^+ ions with 0.5 keV is shown in Fig. 3. It is similar to the XPS depth profile from Fig. 2, taking into account the specificity of both techniques for depth profiling. The selected signals of C_3N^-, CH^-, FeO_2^-, CrO^-, FeH^-, NiH_2^- and CrH_2^- are shown in Fig. 3 for simplicity. The interface width between the polymer film and the substrate is almost the same (about 15 nm) in both the XPS and SIMS depth profiles. As already mentioned, the interface thickness is explained by a

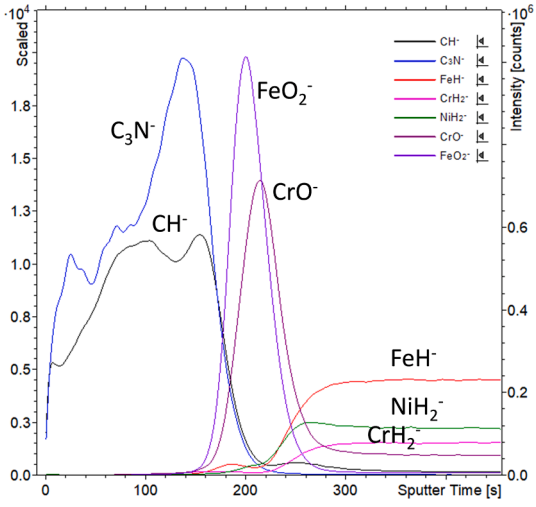

Fig. 3. ToF-SIMS depth profile of negative secondary ions across a polymer film of thickness 70 nm.

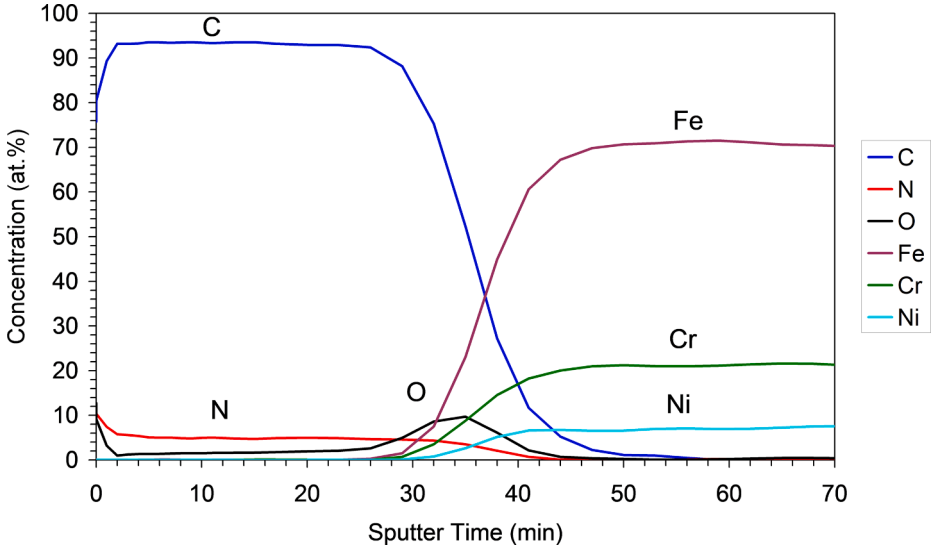

Fig. 2. XPS depth profile across the polymer film of thickness 70 nm.

rough stainless-steel surface due to incomplete polishing rather than the formation of a diffused layer. The ToF-SIMS profile clearly shows the presence of C_3N^- and CH^- signals related to the amine and hydrocarbon groups in the deposited film. Variation of these signals is probably related to a change of ionization due to the matrix effect. At the interface, it can be recognized a thin oxide layer from the FeO_2^-, CrO^- signals. A steel matrix beneath the oxide layer is evidenced in the SIMS profile by the FeH^-, NiH_2^- and CrH_2^- signals. These metal-hydrogen clusters are formed from the emitted metallic ions and hydrogen molecules introduced in the vacuum at the pressure range of 10^{-5} Pa. This is a new approach to reduce a matrix effect in ToF-SIMS depth profiling by flooding the analyses chamber with H_2 gas. We should note that ToF-SIMS is not a quantitative method and that the intensity of signals does not directly reflect the concentration of corresponding species.

The samples were also characterized by GDOES using two different gases introduced into the discharge unit, either pure Ar or a mixture of 96 vol% Ar and 4 vol% O_2. A typical GDOES depth profile of a 500-nm-thick polymer layer when using pure argon for the sample's plasma sputtering is shown in Fig. 4. The discharge parameters adopted for this depth profile were as follows: gas pressure of 450 Pa, discharge power of 20 W, a duty cycle of 0.25, and repetition frequency of 2500 Hz. The evolution of the optical signals for C, N, O, Fe, Cr, and Ni are shown in Fig. 4. The intensity of the Cr and Fe signals was much larger than any other spectral line, so the other elements were multiplied by 50–100 to better read the depth profile.

To evaluate the surface morphology developed during etching, we analyzed the surface of a sample with a polymer thickness of 500 nm after 50 s of etching in the GDOES instrument, when approximately half of the layer thickness was removed (Fig. 4). A typical AFM image is shown in Fig. 5. We can observe round pits of about 65 nm in diameter and 10 nm in height. The roughness on this surface was measured to be about 3.2 nm. A possible reason for such structure may be inhomogeneous plasma distribution above the dielectric layer of polymer on the nanoscale or internal heterogeneity of the polymer layer. At this point, we are not able to explain this in more detail, and this would require further research. The sputtering rate of the polymer layer was evaluated to be about 3.3 nm/s, much faster than for similar XPS and SIMS analysis. The concentrations of C and N were almost constant across the polymer film in accordance with observations by XPS (Fig. 2). The behavior of the elements at the interface between the polymer film and substrate, however, deviates significantly. While the interface thickness in the case of both the XPS and SIMS depth profiles was about 15 nm, it was well over 100 nm in the case of GDOES. Namely, both carbon and

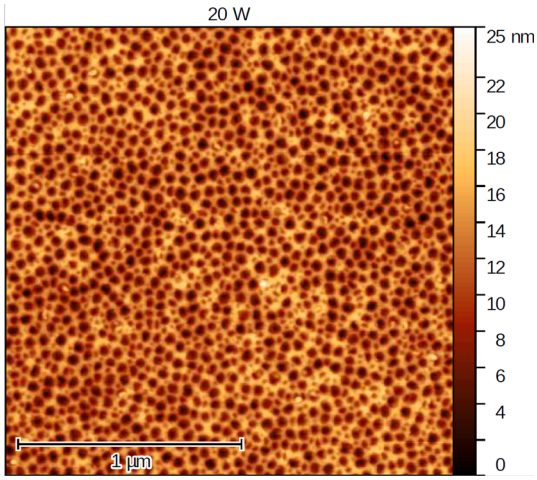

Fig. 5. A typical AFM image of a sample of polymer thickness 500 nm at 30 W and 50 s treatment time in Ar), when a half of the polymer layer was removed in order to reveal development of the surface morphology.

nitrogen lines remained intensive after the Fe and Cr lines prevailed in the optical spectrum. This effect could be attributed either to the retention of carbon and nitrogen in the discharge chamber of the GDOES or highly inhomogeneous etching of the polymer film upon depth profiling, or both. The version of the GDOES instrument used in this study is equipped with a sophisticated pumping system, so any gaseous molecules formed upon etching of the polymer film will be pumped from the discharge chamber quickly. The depth profile in Fig. 4, however, reveals that a substantial concentration of C and N remains about 100 s after the appearance of the Fe and Cr lines. There are two feasible explanations for the persistence of N and C in the optical spectra: 1 – carbon and nitrogen-containing molecules desorb from surfaces other than the substrate in plasma conditions, and 2 – some polymer persists on the sample surface well after a part of the surface was free from polymer.

Details about the discharge and plasma properties in the GDOES instrument adopted in this study are not available. The Ar ions are accelerated in the sheath between the bulk plasma and the sample and bombard the surface. The bombardment causes the depletion of hydrogen in the polymer film and sputtering of the surface atoms. The removed material enters the gaseous plasma, where the atoms are

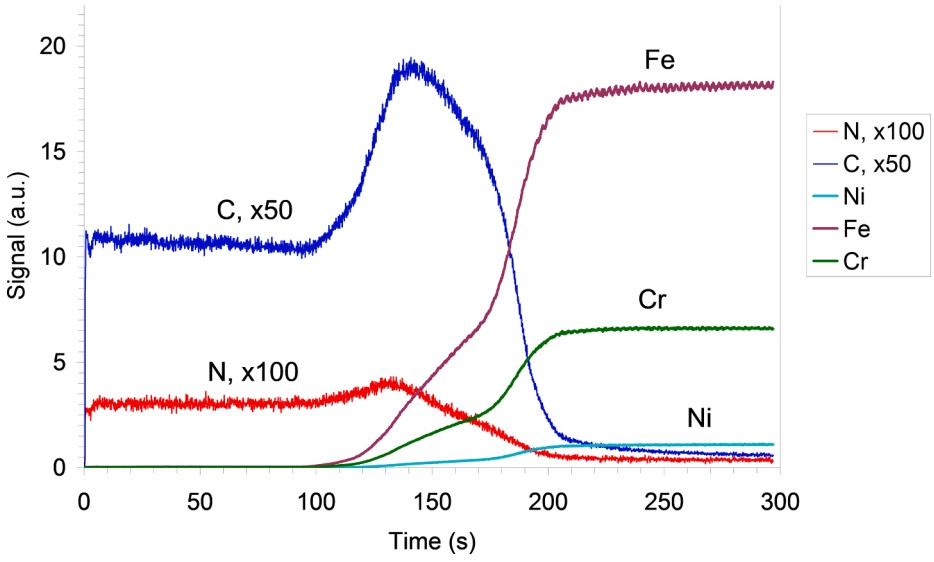

Fig. 4. GDOES depth profile across the polymer film of thickness 500 nm at 20 W using pure Ar.

excited in collisions with the plasma electrons or with the Ar metastables. Although the pressure in the discharge chamber is rather large (450 Pa in the case of the depth profile shown in Fig. 4), not all the removed molecules or atoms are pumped away. Some diffuse inside the gaseous plasma and eventually reach the surface of the counter-electrode. The mean free path of the gaseous molecules at a pressure of 450 Pa is below 0.1 mm, so the removed material suffers numerous collisions in the gas phase until it reaches the surface of the counter-electrode. Residual gases will not be retained significantly on the surface, but radicals such as CH_x ($x < 3$) will stick to any surface facing plasma, causing the formation of a hydrogenated carbon film. This film would remain on the counter-electrode surface forever unless the surface is subjected to bombardment with plasma ions. This effect cannot be evaluated due to the lack of information on discharge coupling and thus an inability to estimate the kinetic energy of ions bombarding the counter-electrode. Another reason for the removal of such unwanted deposits is desorption at very high temperatures, but this effect can be excluded since it is believed that the counter-electrode remains reasonably close to room temperature during the depth profiling.

Another explanation for persistent carbon in the optical spectra long after the Fe and Cr lines appeared is the laterally inhomogeneous etching of the polymer film under bombardment with Ar ions. It is well known that with a non-homogenous sputtering flux during the etching in the GDOES, a crater on the substrate may be formed with a non-flat bottom. This effect deteriorates the depth resolution and the sharpness of the measured interface for thin-film structures like in our case as it was modeled by one of the authors [10].

A third explanation could be a simple shrinkage of the polymer film upon depth profiling due to pure thermal effects. Elevated temperatures cause the melting of a thin polymer film and thus the formation of polymer droplets. As shown in Fig. 1, the polymer temperature is close to 100 °C during the GDOES depth profiling.

To evaluate the morphology at the interface between the polymer film and the steel substrate, the etching in pure Ar was stopped after reaching the interface. The micrograph obtained by the optical microscope and the line profile obtained by profilometry of the bottom of the crater after etching are presented in Figures S1 and S2. These data are shown for the 500-nm thick polymer film. The shape of the crater after pure Ar etching is relatively flat but contains many small dots of 200 – 400 nm in height. As supposed, the origin of the dots after pure Ar etching may be due to the redeposition of the sputtered material from the polymer film or from the deposit on the counter electrode.

Whatever the reason, the persistence of the C and N emission lines in the depth profiles well after the metal lines have appeared represents a serious drawback of GDOES compared to XPS or SIMS. Modern GDOES instruments are also equipped with other gases for the depth profiling of polymer films. The instrument used in this work enables depth profiling using a mixture of Ar and O_2, in particular 96 vol% Ar and 4 vol% O_2. Such a mixture was used as an alternative to pure Ar for the depth profiling of our samples. The addition of oxygen to the Ar plasma complicates the plasma kinetics since there are numerous additional gas-phase and surface reactions involved. The literature on plasma parameters in such gas mixtures is abundant, but we found no paper on plasma parameters in the discharge configuration as adopted by our GDOES instrument. The closest study in terms of similar discharge power density (power per unit volume), similar diameter and length of the discharge tube, and similar pressure and gas mixture was published by Kutasi et al. [18]. She found the most abundant species to be metastable neutral O_2 molecules in the singlet state, followed by neutral oxygen atoms in the ground state. The concentration of Ar^+ ions and Ar metastables was much smaller (the order of magnitude was 10^{17} m^{-3}), while the concentration of oxygen ions (molecular or atomic) was at least an order of magnitude lower. In any case, the flux of the reactive oxygen species suitable for chemical interaction with polymer films on any surface facing plasma is much larger than the flux of positive ions in discharge configurations similar to that of our GDOES instrument.

Fig. 6 shows a typical GDOES depth profile for plasma created in a mixture of 96% Ar + 4% O_2. As compared to Fig. 4, which shows the depth profile of the same sample under the same conditions but using Ar only, we observe two important differences: 1 – the removal of the polymer film is much faster, and 2 – neither carbon nor nitrogen persist in the optical spectra once the Fe and Cr lines have become significant. The sputtering rate was estimated to be about 83 nm/s in comparison to the sputtering rate of 3.3 nm/s when profiling in pure Ar. The fast sputtering of the polymer film in a mixture of Ar + O_2 gases is attributed to chemical etching of the carbon-containing material rather than sputtering and will be elaborated later in this paper. The interface is far less broad in the case of the oxygen admixture than when using only argon for the depth profiling. Therefore, the application of oxygen in the gaseous plasma suitable for etching of the sample for depth profiling eliminates both the nitrogen and carbon lines from the optical spectra once the signals from the metal ions become noticeable. As explained above, the carbon may persist in the spectra when only Ar is used for the depth profiling either due to the retention of carbon on the walls of the counter-electrode or due to highly inhomogeneous sputtering. Reactive oxygen species interact chemically with carbon-containing materials causing the formation of simple molecules that quickly desorb from the surfaces, predominantly H_2O, CO and CO_2. The application of oxygen for the depth profiling of thin polymer films on metallic substrates is therefore highly recommended.

To confirm further our assumption we analyzed morphology of the crater obtained by the Ar + O_2 etching by optical microscope and by profilometer what is shown in Figures S3 and S4. The crater shape is less flat than in the case of the pure Ar etching (Figures S1 and S2), but it does not show a presence of dots. The absence of the dots for etching with the Ar + O_2 mixture shows that the redeposition of the sputtered material does not occur. Similar behavior was observed by Takahara et al. performing GDOES etching on the graphite layer in the Ar + O_2 mixture in comparison to etching in pure Ar, where similar dots were observed [13]. The Figure S4 shows that the bottom of crater obtained by the Ar/O_2 mixture etching does not contain dots but there are present regions with pronounced convexity. This morphology may be related with inhomogeneous etching in the Ar/O_2 mixture due to the O_2 addition. Such effect on morphology was also reported by Fernandez et al. applying the Ar/O_2 mixture at similar conditions for etching steel and glass substrates [11].

In order to gain an insight into the mechanisms of interaction between the polymer films and plasma created in either pure Ar or an Ar-O_2 mixture, we performed more systematic depth profiling at various discharge parameters and compared the results with those obtained using Ar only. Fig. 7 compares the etching rate of the 500-nm-thick polymer film versus the gas pressure at a constant discharge power of 30 W for pure Ar and the Ar-O_2 mixture, as deduced from the corresponding GDOES depth profiles. Fig. 8 shows a similar comparison, but for etching rate versus power at a constant pressure of 400 Pa. The repetition frequency of the pulsed RF discharge was 2.5 kHz, and the duty cycle 0.25 for all conditions.

Fig. 7 indicates that the etching rate with gaseous plasma created in pure argon (lower curve) is about 6 nm/s and it remains almost constant in the range of pressures from 400 to 700 Pa. The etching mechanism, in this case, is sputtering by bombardment with Ar ions. The sputtering efficiency depends on the ions' kinetic energy and the flux of ions onto the surface. At low fluences, the sputtering yield decreases with increasing fluence due to various reactions in the surface layer of the polymer film affected by the Ar ions, but after receiving the fluence of about 10^{20} m^{-2} the yield assumes a rather constant value of roughly one carbon atom per incident Ar ion at an Ar^+ energy of 1 keV [27]. Such fluency is achieved in our case in the first second of plasma treatment, so we can assume a rather time-independent sputtering yield of the polymer film. Increasing the pressure causes an increase in the number of gaseous species available for ionization, which should be beneficial for increasing electron density. On the other hand, increasing the pressure

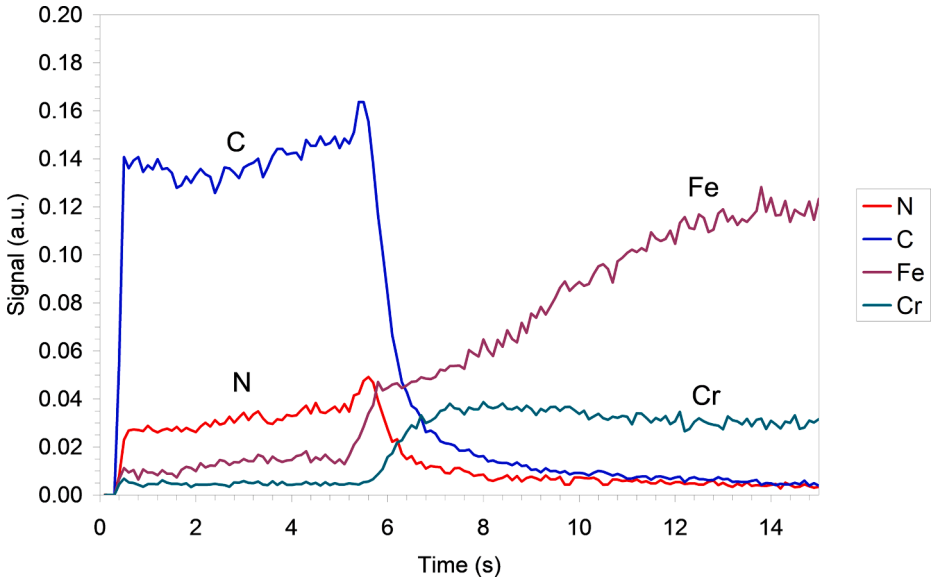

Fig. 6. GDOES depth profile across the polymer film of thickness 500 nm at 20 W using pure Ar + 4% O_2. Oxygen signal was also detected throughout the depth profile but not shown in this Figure.

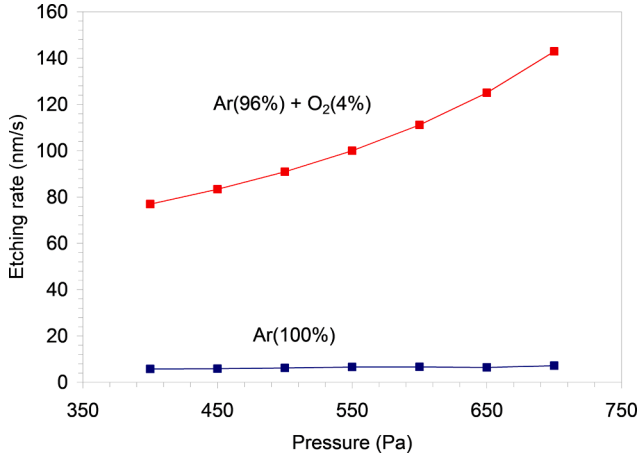

Fig. 7. The etching rate during GDOES depth profiling of the polymer film of thickness 500 nm versus gas pressure at discharge power 30 W using pure Ar (lower curve) and the Ar-4% O_2 mixture (upper curve).

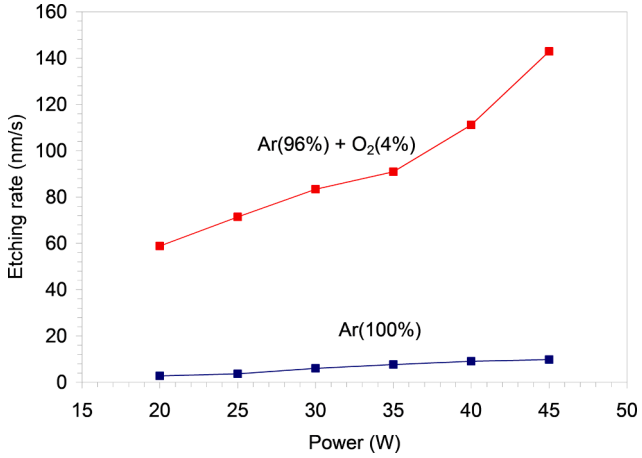

Fig. 8. The etching rate during GDOES depth profiling of the polymer film of thickness 500 nm versus discharge power at pressure 400 Pa using pure Ar (lower curve) and the Ar- 4% O_2 mixture (upper curve).

causes a decrease in the mean free path of the gaseous species, which in turn causes more frequent collisions of the plasma electrons and a higher probability of the loss of the electron energy and correspondingly lower electron temperature. This effect, however, becomes important at pressures much larger than those applied in our experiments, since the power density is large enough to sustain plasma even at an elevated pressure.

A standard presentation of the capacitively coupled plasma involves an equivalent circuit that includes at least two capacitive and a resistive component of the total impedance, although such a presentation may not always be completely accurate, especially when a thin dielectric film persists on the powered electrode [28]. The capacitive components reflect the impedances across the powered and grounded electrodes, and the resistive across the bulk plasma. The current carriers in the bulk plasma are predominantly electrons and, in the sheaths, ions. Since the electron mobility is much larger than the mobility of positive ions (mainly due to the mass differences), the resistive component is usually neglected for short distances between the electrodes like those in the discharge configuration of our GDOES instrument. The key feature of a capacitively coupled discharge as a source of Ar ions is DC self-biasing of the powered electrode that causes a high time-averaged negative bias of the electrode against the bulk plasma. The self-bias slightly decreases with increasing pressure in the range of several 100 Pa [29], but the electron density increases and so does the ion density (plasma is quasi-neutral), so the result of these competing effects is an almost pressure-independent etching rate, as shown in Fig. 7 for pure Ar.

The distribution of Ar ions impinging the sample surface over the kinetic energy is the parameter that governs the sputtering kinetics. Unfortunately, such information is not available. The kinetic energy could be deduced from the RF voltage, but it is not feasible to measure it in our GDOES instrument. The voltage should be large enough to enable gas breakdown. The necessary voltage is estimated from the Paschen curves [30]. Knowing the geometry of the RF discharge chamber in our GDOES instrument, it is possible to conclude that the instrument operates close to the minimum in the Paschen curve, which is just over 100 V for the case of pure argon discharges [30]. If the sheath next to the powered electrode were collisionless, the Ar ions would have been monochromatic at the kinetic energy, which corresponds to the applied voltage. The collision frequency and thus the deviation of the energy distribution from monochromatic could be estimated from the density

and the electron temperature in plasma. However, these parameters are not provided by the GDOES producer, and it is not feasible to measure them in our instrument. From the general knowledge about the behavior of such discharges, we can only speculate that the maximal kinetic energy of Ar ions impinging the samples should be within 100 and 200 eV, but a significant fraction of ions could be less energetic.

The interaction between gaseous plasma and polymer samples is different when oxygen is admixed with argon, as can be seen from the upper curve in Fig. 7. The etching rate versus pressure for the case of 4% O_2 admixture is in the range between 70 and 140 nm/s, and it is an order of magnitude larger than the rate for pure Ar. It is also an almost parabolic increase in the etching rate with increasing pressure for the Ar-O_2 mixture. The effects cannot be explained by more intensive sputtering, but the chemical interaction between reactive gaseous species in an Ar-O_2 plasma and the polymer surface must be taken into account. According to recent review papers [15,31], the major reactive oxygen species in oxygen-containing plasma are neutral oxygen atoms. The O-atoms interact with the polymer surface, causing the formation of oxygen functional groups on the surface. The saturation of the polymer surface with oxygen functional groups is accomplished after achieving a fluence of about 10^{21} m^{-2} [32,33]. The flux of O-atoms onto the polymer surface is

$$j_0 = \frac{1}{4} n_0 \langle v \rangle_0 \tag{2}$$

where n_O is the O-atom density in the plasma next to the polymer surface and $\langle v \rangle_O$ is the average random velocity of O atoms in a gaseous plasma, i.e.

$$\langle v \rangle_0 = \sqrt{\frac{8kT_0}{\pi m_0}} \tag{3}$$

Here, k is the Boltzmann constant, T_O is the temperature of O atoms in the gaseous plasma, and m_O is the mass of an oxygen atom. According to Kutasi et al., the density of O atoms in Ar + 4 vol% O_2 plasma created at the power density of several 10 W cm^{-3} is about 4×10^{20} m^{-3} [18]. The corresponding flux taking into account the gas temperature of 400 K is about 8×10^{22} $m^{-2}s^{-1}$. The time for saturation of the polymer surface with oxygen groups is thus close to 10 ms. Once the surface is saturated, the O-atoms cause chemical etching. The etching rate is

$$\frac{dx}{dt} = \frac{\eta j_O M}{\rho N_A} \tag{4}$$

where η is the probability that an impinging O-atom removes a carbon atom from the polymer surface, M is the molar mass of carbon (using the rough approximation that the entire polymer mass is carbon), ρ is the polymer density, and N_A is the Avogadro number. Taking into account the numerical values, i.e. $j_O = 8 \times 10^{22}$ $m^{-2}s^{-1}$, M = 12 kg $kmol^{-1}$, $\rho = 10^3$ kg m^{-3} and $N_A = 6 \times 10^{26}$ $kmol^{-1}$, and the reaction probability η = 1 we obtain an etching rate of 1.5 μm/s. The measured etching rate for the Ar-O_2 mixture is over an order of magnitude smaller than what can be explained with the above simplifications, so the reaction probability for O-atoms is well below 1. In fact, the reaction probability for O-atoms for a thin polyethylene terephthalate film on a quartz substrate as determined with a quartz-crystal microbalance at room temperature was of the order of 10^{-6} in the case that the polymer was exposed only to O-atoms [34], and between 10^{-4} and 10^{-3} when the polymer was exposed to a weakly ionized oxygen plasma of negligible ion kinetic energy [34]. So, orders of magnitude lower than in the case of our GDOES experiments, where the reaction probability is close to 0.1. The virtual discrepancy is explained by the synergy of the chemical interaction due to polymer oxidation with oxygen atoms and the simultaneous bombardment with Ar^+ ions. The technique is usually called “reactive ion etching” and was commercialized in microelectronics decades ago [35].

The almost parabolic increase of the etching rate with increasing pressure, as evident from Fig. 7 for the Ar-O_2 mixture, is difficult to explain. The etching rate with Ar only does not increase much with increasing pressure. The significant increase of the etching rate as observed in Fig. 7 for the Ar-O_2 mixture should be a consequence of the higher flux of the oxygen reactive species onto the polymer surface. The flux of these species, however, increases at most linearly with increasing pressure, so one would expect a rather linear curve for the Ar-O_2 mixture. In terms of numerical values, the discrepancy is not that dramatic. Although, when the pressure increases from 400 to 700 Pa (by a factor of 1.75), the etching rate increases from 78 to 148 nm/s (by a factor of 1.9).

The discharge power affects the etching rate much more than the pressure. Fig. 8 illustrates this effect for pure Ar and for the Ar-O_2 mixture. The etching rate increases rather linearly with increasing power, and it is about 15 times higher for the Ar-O_2 mixture compared to the pure Ar gas. This is a result of two effects: 1 – increasing self-bias of the powered electrode, and 2 – increasing ion density in plasma. The first effect causes increased Ar^+ kinetic energy when bombarding the sample, and the second an increased ion flux. Both contribute to more extensive etching and also heating of the polymer surface, but the latter effect does not cause a significant increase in the surface temperature for thin polymer films (see Fig. 1).

Here, it is worth mentioning that the exact mechanisms of oxygen plasma interaction with polymers are still not well understood. The main reactants in oxygen plasmas are usually neutral oxygen atoms. A useful theory on the interaction of O-atoms with a polymer was recently provided by Longo et al. [36]. The authors elaborated on almost 20 reaction paths that lead to surface functionalization at low atom fluence, and etching at larger fluencies. The etching causes bong cleavage, so it is likely that low-molecular-mass fragments are also formed on the polymer surface. The fragments may be released upon low-pressure conditions so that incomplete oxidation may occur. The theoretical predictions provided by Longo were recently confirmed by experiments using a broad range of O-atom fluences [37]. Gaseous plasma, sustained in a mixture of argon and oxygen, comprises other species but neutral atoms. The synergy between the reactive species is not understood, especially because such a plasma is a rich source of vacuum ultraviolet (VUV) radiation [38], which is renowned for its ability to break bonds in the surface film of organic materials [39].

4. Conclusions

Characterization of thin polymer films on stainless-steel substrates by GDOES using either pure argon or a mixture of argon with 4 vol% oxygen provided an insight into the phenomena that take place on the surface of samples during etching. The etching rates were by a factor of around 15 larger in the case that oxygen was added to the plasma created in the GDOES instrument, as compared to classic etching by sputtering of the polymer film with Ar ions. Such a pronounced effect was explained by a synergy between the reactive oxygen species that interact chemically with the polymer surface and the bombardment with Ar ions. A rough estimation of the plasma parameters taking into account the available scientific literature, made it possible to estimate the probability that an oxygen atom from the gas phase interacts with carbon on the surface of the polymer material. The probability was found to be close to 0.1, which is far larger than what was reported for the interaction of pure oxygen plasma of comparable O-atom density with polymer samples kept at a floating potential so that the kinetic effects caused by bombardment with positively charged ions were negligible.

A peculiarity of GDOES depth profiling when using argon only as the source of polymer etching is the virtual persistence of the carbon signal well after the signals from metallic atoms have become large. Possible explanations for this observation were presented in this paper and briefly discussed. A comparison with depth profiles obtained by XPS and SIMS proved that the persistence of carbon in the depth profiles obtained by GDOES was an artefact of the GDOES method. The problem was

solved effectively by using a mixture of Ar with 4 vol% oxygen, where we observed rather sharp interfaces between the polymer film and metallic substrate. The results, therefore, confirm the superior analytical results when using oxygen in GDOES depth profiles.

CRediT authorship contribution statement

Janez Kovač: Investigation, Writing – review & editing, Conceptualization. **Jernej Ekar:** Investigation. **Miha Čekada:** Investigation. **Lenka Zajíčková:** Investigation. **David Nečas:** Investigation. **Lucie Blahová:** Investigation. **Jiang Yong Wang:** Investigation, Resources. **Miran Mozetič:** Resources, Writing – review & editing, Conceptualization.

Declaration of Competing Interest

The authors declare that they have no known competing financial interests or personal relationships that could have appeared to influence the work reported in this paper.

Acknowledgement

The authors acknowledge the financial support from the Slovenian Research Agency (research core funding No. P2-0082 and project L2-1728), Slovenian-Chinese bilateral project BI-CN/17-18-003. We also acknowledge CzechNanoLab Research Infrastructure supported by MEYS CR (LM2018110) and the project 21-12132 J supported by the Czech Science Foundation

Appendix A. Supplementary material

Supplementary data to this article can be found online at https://doi.org/10.1016/j.apsusc.2021.152292.

References

[1] W. Grimm, Eine neue glimmentladungslampe für die optische emissionsspektralanalyse, Spectrochim. Acta, Part B 23 (7) (1968) 443–454.
[2] V. Hoffmann, M. Kasik, P.K. Robinson, C. Venzago, Glow discharge mass spectrometry, Anal. Bioanal. Chem. 381 (2005) 173–188.
[3] S. Carquigny, B. Lakard, S. Lakard, V. Moutarlier, J.-Y. Hihn, L. Viau, Investigation of pharmaceutically active ionic liquids as electrolyte for the electrosynthesis of polypyrrole and active component in controlled drug delivery, Electrochim. Acta 211 (2016) 950–961.
[4] K. Cysewska, L.F. Macía, P. Jasiński, A. Hubin, In-situ odd random phase electrochemical impedance spectroscopy study on the electropolymerization of pyrrole on iron in the presence of sodium salicylate – The influence of the monomer concentration, Electrochim. Acta 290 (2018) 520–532.
[5] T. Sizun, T. Patois, M. Bouvet, B. Lakard, Microstructured electrodeposited polypyrrole–phthalocyanine hybrid material, from morphology to ammonia sensing, J. Mater. Chem. 22 (2012) 25246–25253.
[6] S. Giaveri, P. Gronchi, A. Barzoni, IPN Polysiloxane-Epoxy Resin for High Temperature Coatings: Structure Effects on Layer Performance after 450 °C Treatment, Coatings 7 (2017) 213.
[7] V. Moutarlier, S. Lakard, T. Patois, B. Lakard, Glow discharge optical emission spectroscopy: a complementary technique to analyze thin electrodeposited polyaniline films, Thin Solid Films (2014) 27–35.
[8] A. Groza, C.S. Ciobanu, C.L. Popa, S.L. Iconaru, P. Chapon, C. Luculescu, M. Ganciu, D. Predoi, Structural Properties and Antifungal Activity against Candida albicans Biofilm of Different Composite Layers Based on Ag/Zn Doped Hydroxyapatite-Polydimethylsiloxanes, Polymers 8 (2016) 131.
[9] A. Surmeian, D.M. Maximean, B. Mihalcea, O. Stoican, B. Butoi, O. Danila, P. Dinca, I. Barbut, L. Tudor, A. Fazacas, GDOES and GDMS analytical systems, effective tools for characterization of conductive and nonconductive material surfaces, University Politehnica of Bucharest, Scientific Bulletin-Series A-Appl. Mathematics. Phys. 77 (2015) 273–280.
[10] Y. Liu, W. Jian, J.Y. Wang, S. Hofmann, K. Shimizu, Quantitative reconstruction of the GDOES sputter depth profile of a monomolecular layer structure of thiourea on copper, Appl. Surf. Sci. 331 (2015) 140–149.
[11] B. Fernández, N. Bordel, R. Pereiro, A. Sanz-Medel, Investigations of the effect of hydrogen, nitrogen or oxygen on the in-depth profile analysis by radiofrequency argon glow discharge-optical emission spectrometry, J. Anal. At. Spectrom. 18 (2) (2003) 151–156.
[12] B. Fernández, N. Bordel, C. Pérez, R. Pereiro, A. Sanz-Medel, The influence of hydrogen, nitrogen or oxygen additions to radiofrequency argon glow discharges for optical emission spectrometry, J. Anal. At. Spectrom. 17 (11) (2002) 1549–1555.
[13] H. Takahara, A. Kojyo, K. Kodama, T. Nakamura, K. Shono, Y.o. Kobayashi, M. Shikano, H. Kobayashi, Depth profiling of graphite electrode in lithium ion battery using glow discharge optical emission spectroscopy with small quantities of hydrogen or oxygen addition to argon, J. Anal. At. Spectrom. 29 (1) (2014) 95–104.
[14] W. Fischer, A. Naoumidis, H. Nickel, Effects of a controlled addition of nitrogen and oxygen to argon on the analytical parameters of glow discharge optical emission spectrometry, J. Anal. At. Spectrom. 9 (3) (1994) 375, https://doi.org/10.1039/ja9940900375.
[15] A. Vesel, M. Mozetic, New developments in surface functionalization of polymers using controlled plasma treatments, J. Phys. D Appl. Phys. 50 (29) (2017) 293001, https://doi.org/10.1088/1361-6463/aa748a.
[16] M. Mozetič, K. Ostrikov, D.N. Ruzic, D. Curreli, U. Cvelbar, A. Vesel, G. Primc, M. Leisch, K. Jousten, O.B. Malyshev, J.H. Hendricks, L. Kövér, A. Tagliaferro, O. Conde, A.J. Silvestre, J. Giapintzakis, M. Buljan, N. Radić, G. Dražić, S. Bernstorff, H. Biederman, O. Kylián, J. Hanuš, S. Milošević, A. Galtayries, P. Dietrich, W. Unger, M. Lehocky, V. Sedlarik, K. Stana-Kleinschek, A. Drmota-Petrič, J.J. Pireaux, J.W. Rogers, M. Anderle, Recent advances in vacuum sciences and applications, Journal of Physics D: Applied Physics 47 (2014) 153001.
[17] M. Mozetič, A. Vesel, G. Primc, C. Eisenmenger-Sittner, J. Bauer, A. Eder, G.H. S. Schmid, D.N. Ruzic, Z. Ahmed, D. Barker, K.O. Douglass, S. Eckel, J.A. Fedchak, J. Hendricks, N. Klimov, J. Ricker, J. Scherschligt, J. Stone, G. Strouse, I. Capan, M. Buljan, S. Milošević, C. Teichert, S.R. Cohen, A.G. Silva, M. Lehocky, P. Humpoliček, C. Rodriguez, J. Hernandez-Montelongo, D. Mercier, M. Manso-Silván, G. Ceccone, A. Galtayries, K. Stana-Kleinschek, I. Petrov, J.E. Greene, J. Avila, C.Y. Chen, B. Caja-Munoz, H. Yi, A. Boury, S. Lorcy, M.C. Asensio, J. Bredin, T. Gans, D. O'Connell, J. Brendin, F. Reniers, A. Vincze, M. Anderle, L. Montelius, Recent developments in surface science and engineering, thin films, nanoscience, biomaterials, plasma science, and vacuum technology, Thin Solid Films 660 (2018) 120–160.
[18] K. Kutasi, V. Guerra, P. Sá, Theoretical insight into Ar–O2surface-wave microwave discharges, J. Phys. D Appl. Phys. 43 (2010), 175201.
[19] A. Manakhov, M. Landová, J. Medalová, M. Michlíček, J. Polčák, D. Nečas, L. Zajíčková, Cyclopropylamine plasma polymers for increased cell adhesion and growth, Plasma Processes Polym. 14 (2017) 1600123.
[20] L. Zajíčková, V. Buršíková, Z. Kučerová, J. Franclová, P. Sťahel, V. Peřina, A. Macková, Organosilicon thin films deposited by plasma enhanced CVD: Thermal changes of chemical structure and mechanical properties, J. Phys. Chem. Solids 68 (2007) 1255–1259.
[21] L. Štrbková, A. Manakhov, L. Zajíčková, A. Stoica, P. Veselý, R. Chmelík, The adhesion of normal human dermal fibroblasts to the cyclopropylamine plasma polymers studied by holographic microscopy, Surf. Coat. Technol. 295 (2016) 70–77.
[22] A.T. Patrick Chapon, Célia Olivero, Tatsuhito Nakamura, Hiroko Nakamura, Akira Fujimoto, Method of measuring a solid organic or polymer sample by luminescent discharge spectrometry, in: E.P. Office (Ed.), 2016.
[23] M. Michlíček, L. Blahová, E. Dvořáková, D. Nečas, L. Zajíčková, Deposition penetration depth and sticking probability in plasma polymerization of cyclopropylamine, Appl. Surf. Sci. 540 (2021), 147979.
[24] I. Nemcakova, L. Blahova, P. Rysanek, A. Blanquer, L. Bacakova, L. Zajíčková, Behaviour of Vascular Smooth Muscle Cells on Amine Plasma-Coated Materials with Various Chemical Structures and Morphologies, Int. J. Mol. Sci. 21 (2020) 9467.
[25] A.M. Ektessabi, S. Hakamata, XPS study of ion beam modified polyimide films, Thin Solid Films 377–378 (2000) 621–625.
[26] T. Miyayama, N. Sanada, S.R. Bryan, J.S. Hammond, M. Suzuki, Removal of Ar+ beam-induced damaged layers from polyimide surfaces with argon gas cluster ion beams, Surf. Interface Anal. 42 (2010) 1453–1457.
[27] J. Zekonyte, V. Zaporojtchenko, F. Faupel, Investigation of the drastic change in the sputter rate of polymers at low ion fluence, Nucl. Instrum. Methods Phys. Res., Sect. B 236 (2005) 241–248.
[28] T.S. Ho, C. Charles, R. Boswell, Redefinition of the self-bias voltage in a dielectrically shielded thin sheath RF discharge, J. Appl. Phys. 123 (2018), 193301.
[29] P. Saikia, H. Bhuyan, M. Escalona, M. Favre, R.S. Rawat, E. Wyndham, A nonlinear global model of single frequency capacitively coupled plasma and its experimental validation, AIP Adv. 8 (2018), 045113.
[30] W. contributors, Paschen's law, in, Wikipedia, The Free Encyclopedia.
[31] M. Mozetič, G. Primc, A. Vesel, R. Zaplotnik, M. Modic, I. Junkar, N. Recek, M. Klanjšek-Gunde, L. Guhy, M.K. Sunkara, M.C. Assensio, S. Milošević, M. Lehocky, V. Sedlarik, M. Gorjanc, K. Kutasi, K. Stana-Kleinschek, Application of extremely non-equilibrium plasmas in the processing of nano and biomedical materials, Plasma Sources Sci. Technol. 24 (2015), 015026.
[32] T. Vukušić, A. Vesel, M. Holc, M. Ščetar, A.R. Jambrak, M. Mozetič, Modification of Physico-Chemical Properties of Acryl-Coated Polypropylene Foils for Food Packaging by Reactive Particles from Oxygen Plasma, Materials 11 (2018) 372.
[33] A. Vesel, R. Zaplotnik, J. Kovac, M. Mozetic, Initial stages in functionalization of polystyrene upon treatment with oxygen plasma late flowing afterglow, Plasma Sources Sci. Technol. 27 (2018), 094005.
[34] A. Vesel, M. Kolar, A. Doliska, K. Stana-Kleinschek, M. Mozetic, Etching of polyethylene terephthalate thin films by neutral oxygen atoms in the late flowing afterglow of oxygen plasma, Surf. Interface Anal. 44 (2012) 1565–1571.

[35] V.M. Donnelly, A. Kornblit, Plasma etching: Yesterday, today, and tomorrow, J. Vac. Sci. Technol., A 31 (5) (2013) 050825, https://doi.org/10.1116/1.4819316.
[36] R.C. Longo, A. Ranjan, P.L.G. Ventzek, Density Functional Theory Study of Oxygen Adsorption on Polymer Surfaces for Atomic-Layer Etching: Implications for Semiconductor Device Fabrication, ACS Appl. Nano Mater. 3 (6) (2020) 5189–5202.
[37] A. Vesel, R. Zaplotnik, M. Mozetič, G. Primc, Surface modification of PS polymer by oxygen-atom treatment from remote plasma: Initial kinetics of functional groups formation, Appl. Surf. Sci. 561 (2021), 150058.
[38] D. Popović, M. Mozetič, A. Vesel, G. Primc, R. Zaplotnik, Review on vacuum ultraviolet generation in low-pressure plasmas, Plasma Processes Polym. 18 (2021) 2100061.
[39] Y. Zhang, K. Ishikawa, M. Mozetič, T. Tsutsumi, H. Kondo, M. Sekine, M. Hori, Polyethylene terephthalate (PET) surface modification by VUV and neutral active species in remote oxygen or hydrogen plasmas, Plasma Processes Polym. 16 (2019) 1800175.